Drought Monitoring Using MODIS Satellite-Based Data in Kamphaeng Phet Province, Thailand

Preedapirom, P.,[1] Robert, O. P.,[1*] Onchang, R.[1] and Jeefoo, P.[2]
[1]Department of Environmental Science, Faculty of Science, Silpakorn University (Sanamchandra Campus), Thailand, E-mail: preedapirom_p@su.ac.th, robert_o@silpakorn.edu,* rattapon.onchang@gmail.com
[2]Geographic Information Science, School of Information and Communication Technology, University of Phayao, Thailand, E-mail: phaisarn.je@up.ac.th
**Corresponding Author*

DOI: https://doi.org/10.52939/ijg.v20i1.3019

Abstract
Drought is a lengthened dry period in natural climate pattern which is one of the top global concerns. Drought in Thailand has been a long occurring issue affecting serious impact on health, economy, energy, and especially agricultural sector. Less precipitation caused long term water levels by lowering river volume and underground water. Therefore, the drought problem in Thailand is becoming more frequent and more severe. Kamphaeng Phet province located at the upper central part of Thailand demonstrated as the most drought-prone area. The objective of this study was to develop an approach for drought monitoring in provincial scale. MOD13Q1 dataset retrieved from MODIS satellite passing in different periods of Kamphaeng Phet was employed to develop the approach. Normalized Vegetation Index (NDVI) was extracted from the MOD13Q1 dataset so as to detect the vegetation condition of the study area. Afterwards NDVI was essentially standardized into Standardized Vegetation Index (SVI) in order to examine the area where NDVI was different from average value (Deviation). The probability of SVI acquired from NDVI standard scores reflected vegetation states explaining density and drought of vegetation in each period of time and season. Time series analysis of drought was implemented using SVI variances in different seasons. Additionally, precipitation variable was also included to find statistical consistency between SVI and precipitation. The lowest average of SVI was referred as drought, and nearly 0 value described severe drought. It was found that the most severe drought of Kamphaeng Phet occurred in 2020. In 2021, 2019, and 2018 drought showed at severe, moderate, and low level, respectively. Using both NDVI and SVI approach can be applied for drought monitoring and mitigation. Preparedness measures and public awareness of drought mitigation in this area can be enhanced.

Keywords: Drought, MOD13Q1, Spatio-Temporal Analysis, Normalized Vegetation Index, Standardized Vegetation Index Variance

1. Introduction

A drought was natural water deficiency from delayed rain and unseasonable rainfall [1]. Drought is one of the natural disorders that can bring hazards to million numbers of people every year, mostly affected the agrarian community, similarly decrease the food production substantially which leads to the great effects on the country economy as well as the food supply chain system [2]. Drought is really a complex phenomenon whose severity and extent not only depends on the spatial and temporal distribution of rainfall but also on other hydro-meteorological and agricultural factors [3] and [4].

The study area focused to be investigated drought is one of the drought prone areas. Drought disrupts the whole system in plantation and agricultural practices. Due to the lack of water, the plants cannot grow properly resulting in drastic decline in crop yield. People in the drought prone areas even migrate to other places in search of works when they don't acquire good turn over. This is in the long run causing social security problems to the country. One of the main natural disasters that has an impact on the environment and economies of nations all over the world is drought.

Monitoring dry spells using weather data alone is insufficient, especially because weather data might be delayed, sporadic, and partial and do not provide a complete, current picture of the drought conditions [5][6] and [7]. Temperature increases along with changed precipitation patterns cause extreme weather events like droughts, which have a significant impact on agricultural output [8]. Remote Sensing will provide objective and reliable information that could be useful for solving the environmental detection such as air pollution detection [9], burnt detection [10] and [11]. The ability to combine data from various sources to create new knowledge and the inherent visualization (mapping) functions of geosciences make them potentially powerful tools for disaster management. These factors can encourage innovative problem solving and wise decisions that have long-lasting effects on people's lives [12] and [13]. It has been acknowledged that current climate change processes play a significant role in land degradation [1]. In addition to altering the seasonality and amount of precipitation, global warming also affects land surface water balances by altering the atmospheric evaporative demand, which will probably rise in the ensuing decades due to rising air temperatures and a greater vapor pressure deficit. Future droughts are predicted to become more frequent and severe due to climate change, which could prolong the current land degradation and introduce new processes in semi-arid areas [14]. The National Disaster Department of Thailand reported that in lower northern and upper central regions of Thailand drought demonstrated at high level increasingly over past five years [15].

Additionally, the Meteorological Department of Thailand was aware of extreme temperature increase resulting in climate change. Kamphaeng Phet province is one of the areas where drought ought to be monitored. To the best of our knowledge, no published papers have proposed drought monitoring approach of Kamphaeng Phet province, which spatio-temporal patterns of SVI and rainfall intensity was taken into account. To fill this gap, Kamphaeng Phet province was designated as our study area. The objective of this research was to standardize, the Normalized Difference Vegetation Index (NDVI), extracted from MOD13Q1/MODIS dataset to augment drought-monitoring approach. The NDVI based on 16-day calculation was transformed into Standardized Vegetation Index (SVI) describing the probability of vegetation condition deviation. Multi-temporal and spatial drought analysis of Kamphaeng Phet province was performed from 2018 to 2021. The correlation of SVI and precipitation variable was implemented to discover statistical consistency between SVI and precipitation. Using NDVI, SVI and precipitation dataset could be made use of drought monitoring approach explained in this study.

2. Materials and Methods

2.1 Study Area: Kamphaeng Phet Province, Thailand

The province of Kamphaeng Phet, in upper central Thailand, served as the study area (See Figure 1), where regional food supplies were located, and drought had been the most profound effect on the way of living and regional economy [16]. Kamphaeng Phet province comprises 11 districts. The province is 8,607 square kilometers in size and is situated between 18°00' N and 16°40' N and 99°520' E and 101°00' E. Main river is called Ping river passing towards the East of Kamphaeng Phet. In the western part is mountainous and covered with forest land use type with an approximate elevation of 107 meters above mean sea level. Methodology of this paper is illustrated as seen in Figure 2.

2.2 Data

The MODIS/Terra satellite-based data was designated to investigate drought monitoring. In general, tracking and monitoring of natural resources and the environment are done using MODIS/Terra data [17] and [18]. The spatial resolution of MODIS/Terra was 250 – 1000 meters including 36 spectral band recording. The MODIS/Terra made it possible to monitor earth within two days, hence the MODIS/Terra satellite-based data was appropriate for spatio-temporal analysis referred to as change detection. The MODIS dataset known as MOD13Q1 data products was retrieved from section 1; h27v07 (see Figure 1) under geographic coordinate system of UTM WGS 1984 zone 47 N. Time series of MOD13Q1 data from 2018 to 2021 were gathered for further investigation as explained followings.

2.2.1 The Normalized Vegetation Index (NDVI)

NDVI was extracted from MOD13Q1 data products. Equation 1 explained how NDVI was calculated based on the different between electromagnetic reflection of RED and NIR bands [19][20] and [21].

$$NDVI = \frac{NIR - RED}{NIR + RED}$$

Equation 1

The NDVI values were found to range from -1 to +1. The water area's NDVI displayed a negative value [22].

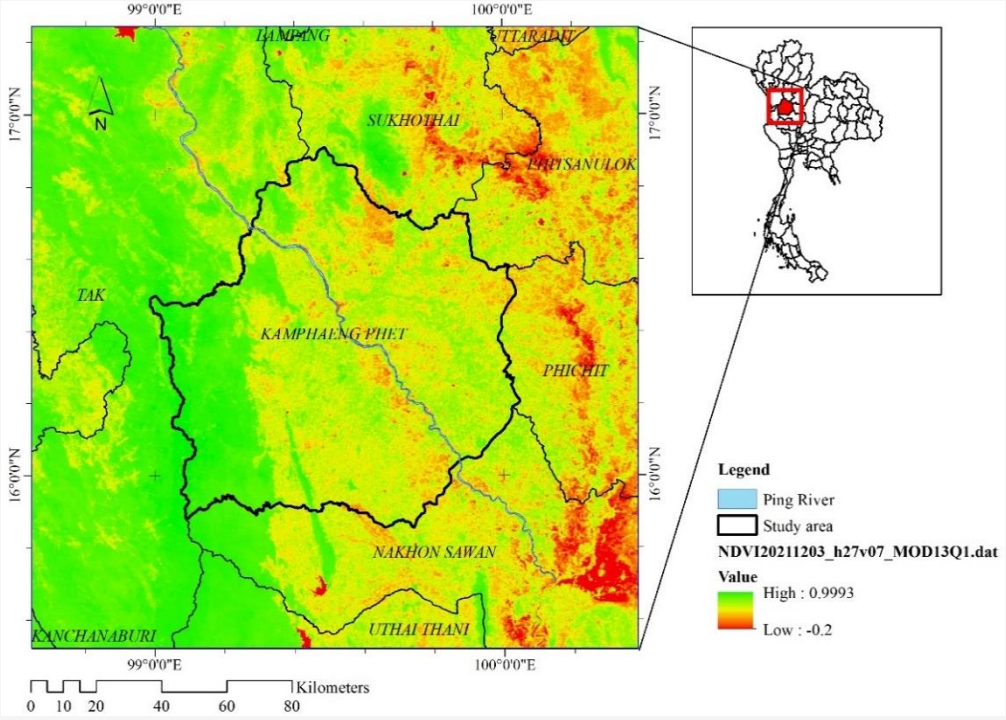

Figure 1: Kamphaeng Phet province, Thailand

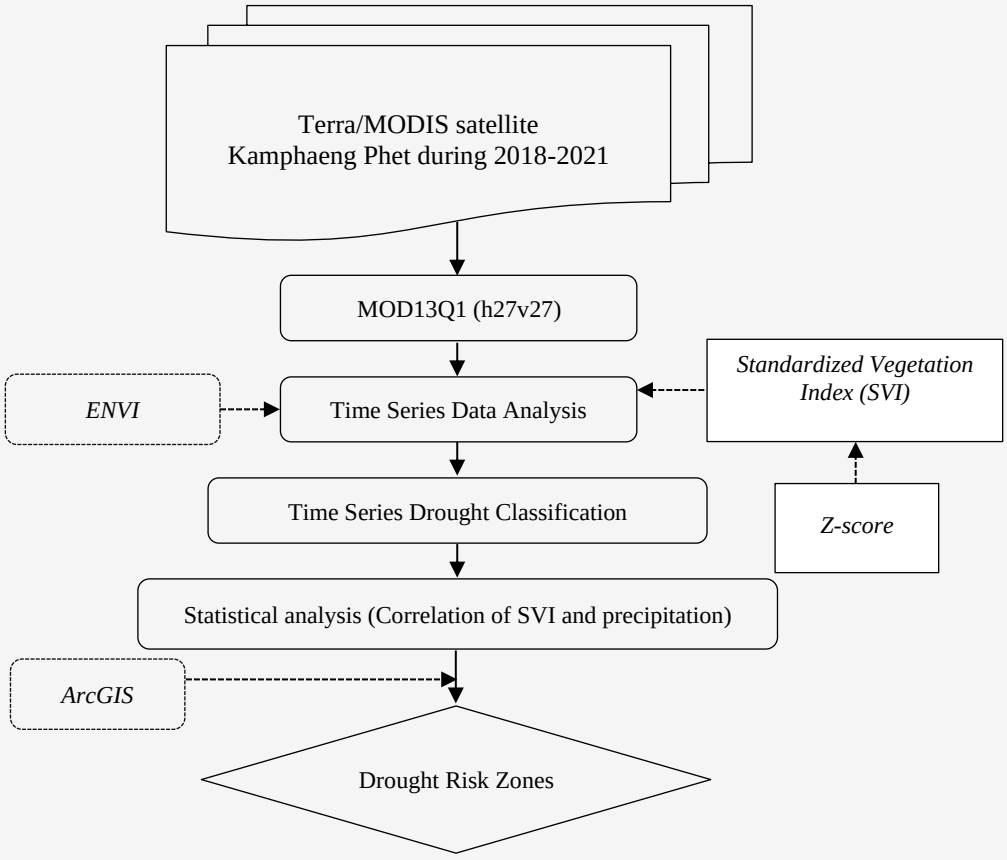

Figure 2: Methodology framework

The NDVI value of the land area with less vegetation was shown to be almost 0. On the other hand, the vegetation area's NDVI was shown as +1. One may draw the conclusion that NDVI data was a useful tool for assessing and projecting changes in vegetation that were influenced by the environment [23] and [24].

2.2.2 The Standardized Vegetation Index (SVI)

The Standard Vegetation Index approach was one technique that might be used to monitor drought. This method is predicated on the likelihood of vegetation at certain points in time. Utilizing a z-score that describes the NDVI deviation, the SVI is computed. According to [25], the Enhanced Vegetation Index (EVI) and the NDVI can both be utilized to calculate the SVI. In this instance, the z-score computation was utilized to determine the NDVI deviation that happened in the assigned month and how it differed from other deviations in the same month in comparison to previous years. Positive z-score values were greater than normal z-score values, whereas negative values were lower than standard z-score values [26]. Equation 2 can be used to obtain the standard z-score.

$$Z_{ijk} = \frac{NDVI_{ijk} - \overline{NDVI}_{ijk}}{\sigma_{ij}}$$

Equation 2

Where:

Z_{ijk} = z-value for pixel *i* during week *j* of year *k*

$NDVI_{ijk}$ = weekly NDVI value for pixel *i* during week *j* of year *k*

$\overline{NDVI}_{ijk}$ = mean NDVI for pixel *i* during week *j* over n year

σ_{ij} = standard deviation of pixel *i* during week *j* over n years

To experiment with all the points in the photos for every season from 2018 to 2021, the Z_{ijk} was assumed to be a standard normal distribution with an average value of 0 and a standard deviation of 1. Equation 3 illustrates how the probability of SVI derived from the NDVI standard scores represented the states of the vegetation [1][20] and [27].

$$SVI = \frac{Z_{ijk} - Z_{ijMIN}}{Z_{ijMAX} - Z_{IJMIN}}$$

Equation 3

Where:

Z_{ijk} = z-value for pixel *i* during month *j* of year *k*

Z_{ijMAX} = maximum of z-value for pixel *i* during month *j*

Z_{ijMIN} = minimum of z-value for pixel *i* during month *j*

The probabilities of vegetation index in the images were illustrated as SVI index, which described probabilities of present vegetation using previous vegetation state. SVI values were $0 < SVI < 1$ in range; 0 explained the lowest standard score of SVI calculated from imagery of 2018-2021. This study drought was categorized into 5 levels using SVI values as seen in Table 1. Each SVI value was found between 0 and 1. Accordance with SVI values in range, vegetation density was considered from very high to very low, respectively.

2.3 SVI Analysis for Drought Monitoring

The SVI computation was performed using monthly SVI data for the years 2018, 2019, 2020, and 2021. It was then essential to determine the average and standard deviation of the SVI values observed in each image. Equation 3 explains that the standard scores for every month and year were needed for the SVI computation. A more thorough analysis of the monthly probability in each SVI site was conducted. The monthly SVI maps of 2018, 2019, 2020, and 2021 were categorized into five classes-based SVI values.

2.4 Software

MS Excel, ENVI version 5.2 and ArcGIS version 10.8 were used in this study. Linear correlation of rainfall and SVI was calculated using MS Excel. ENVI version 5.2 was carried out to investigate drought as mentioned in previous section. ArcGIS version 10.8 was applied for spatial analysis and mapping.

Table 1: The vegetation levels

Drought level of SVI	Percentage of SVI (%)	Vegetation density
1.00 – 0.95	96 - 100	Very high
0.95 – 0.75	76 - 95	High
0.75 – 0.25	26 - 75	Moderate
0.25 – 0.05	6 - 25	Low
0.05 – 0.00	0 - 5	Very low

3. Results and Discussion

3.1 NDVI Calculation

The MODIS satellite-based data retrieved from https://ladsweb.modaps.eosdis.nasa.gov/ was analyzed to identify NDVI information explaining the differences of vegetation density varied from -1 to 1. The average NDVI value was corresponded to density and drought of vegetation in each period of time and season. Table 2 illustrated the highest and lowest average NDVI values discovered from 2018 to 2021 of in Kamphaeng Phet Province. It was explained that the vegetation density of Kamphaeng Phet province was discovered at moderate level (the highest average NDVI between 0.455-0.488) in winter and rainy season. It was possible to determine from the monthly data for 2018 that the vegetation density in the range of -1 to 1 was represented by the lowest, greatest, average, and standard deviation of the NDVI. The average showed the drought and density of vegetation for every season and time interval. November, the winter season, had the highest average of 0.462, while August, the wet season, had the lowest average of 0.2811.

The lowest, greatest, average, and standard deviation of the NDVI indicated the vegetation conditions in the range of -1 to 1, according to the monthly data for 2019. The average showed the drought and density of vegetation for every season and time interval. Rainy season averages ranged from 0.281 in June (early rainy season) to 0.470 in September (highest) in September. It was possible to determine from the monthly data for 2020 that the vegetation conditions in the range of -1 to 1 were represented by the lowest, greatest, average, and standard deviation of the NDVI. For every time period and season, the average represented the drought and density of vegetation. October, during the early winter season, had the highest average of 0.488, while March had the lowest average of 0.267. The lowest, highest, average, and standard deviation of the NDVI indicated the vegetation conditions in the range of -1 to 1, according to the monthly data for 2021. The average showed the drought and density of vegetation for every season and time interval. The winter season's highest average, 0.455, was recorded in November, while the lowest, 0.285, was recorded in March.

3.2 SVI Calculation

The differences of SVI from 2018 to 2021 were calculated. Vegetation states were reflected in the probability of SVI derived from the standard scores of the NDVI. In order to depict vegetation density, the highest and lowest average SVI values were changed from 0 to 1. As shown in Table 3, SVI values indicated vegetation density and drought for each time period and season. The Standard Vegetation Index was used to monitor droughts by reflecting vegetation probability over a range of time periods. Calculations were made to determine the variations in SVI for each image point and period during each year. According to the findings, the vegetation density in 2018 was represented by the lowest, greatest, average, and standard deviation of SVI, which ranged from 0 to 1. The average showed the drought and density of vegetation for every season and time interval. October 16, 2018, the start of the early winter season, had the highest average of 0.466, while August, the rainy season, had the lowest average of 0.281. The averages, or SVI standard scores, determined the SVI variances for every season and time period.

Table 2: The highest and lowest average NDVI values

Data (Year)	The highest and lowest average NDVI			
	The highest	**Month (Season)**	**The lowest**	**Month (Season)**
2018	0.462	November (Winter)	0.281	August (Rainy)
2019	0.470	September (Rainy)	0.281	June (Rainy)
2020	0.488	October (Winter)	0.267	March (Summer)
2021	0.455	November (Rainy)	0.265	March Summer)

Table 3: The highest and lowest average SVI values

Data (Year)	The highest and lowest average SVI			
	The highest	**Month (Season)**	**The lowest**	**Month (Season)**
2018	0.466	October (Winter)	0.281	August (Rainy)
2019	0.470	September (Rainy)	0.287	April (Summer)
2020	0.492	October (Winter)	0.267	March (Summer)
2021	0.455	August (Rainy)	0.267	March Summer)

The vegetation density in 2019 was indicated by the lowest, greatest, average, and standard deviation of SVI, which ranged from 0 to 1. The average showed the drought and density of vegetation for every season and time interval. During the wet season in September, the highest average was 0.470, and the lowest was 0.287 in April. The averages, SVI standard deviation, and the lowest and highest standard scores determined the SVI variances for each season and time period. 2020 saw a range of 0 to 1 for vegetation density, indicated by the lowest, maximum, average, and standard deviation of SVI. For every time period and season, the average represented the drought and density of vegetation. The previous rainy season's highest average, 0.492, was recorded in October, while the lowest, 0.267, was recorded in March. Each season's and period's SVI variances were determined using the averages, SVI standard deviation, and lowest and highest standard scores. The vegetation density in the range of 0 to 1 was represented by the lowest, maximum, average, and standard deviation of SVI in 2021. The average showed the drought and density of vegetation for every season and time interval. During the wet season in August, the highest average was 0.455, and the lowest was 0.267 in March. The averages, SVI standard deviation, and the lowest and highest standard scores determined the SVI variances for each season and time period.

3.3 Multi-temporal Drought Analysis

The temporal variation of the SVI average values was correlated with monthly rainfall, as seen by Figure 3, which shows the SVI monthly average and rainfall over a four-year period. Because vegetation was planted after enough water, SVI changed more slowly than rainfall. In 2018, rainfall variations were lowest in January and February, at that time increased steadily. In September, rainfall level was reached to 944 mm., and throw down to the lowest level in December at 30.6 mm. In 2019, rainfall variations were discovered at the lowest level in March (16 mm.), then increased gradually and reached to 1,080.9 mm in May. Similar to the result in 2018, rainfall was fell to the lowest level at 0.1 mm. In 2020, rainfall differences were slightly reached to the highest level in June (940.9 mm.), then throw down to 752.5 mm. in August. It was increased gradually and reached to highest level at 1,243.1 mm. in September. Subsequently it was dropped progressively and reached to the lowest rainfall level at 0.0 mm. in December. In 2021, rainfall variations were slightly increased to the highest level in April (1,264.3 mm.), and dropped to 377.3 mm. in June. Afterwards, it was increased steadily and reached to 2,786.9 mm. in September, then fell steadily and reached to the lowest level (0.2 mm) in December.

3.4 Statistical Correlation Analysis

SVI variation was shown to be consistent with rainfall amount based on statistical correlation study results between SVI (independent variable) and rainfall (dependent variable) from 2018 to 2021 (see Table 4), which was similar to the study of Liu, and Zhou [28]. Liu, and Zhou [28] investigated spatio-temporal dynamics of drought events using rainfall and NDVI-based drought indicators. The results of statistical correlation analysis between SVI and rainfall from 2018 to 2021 were displayed as seen in Table 4.

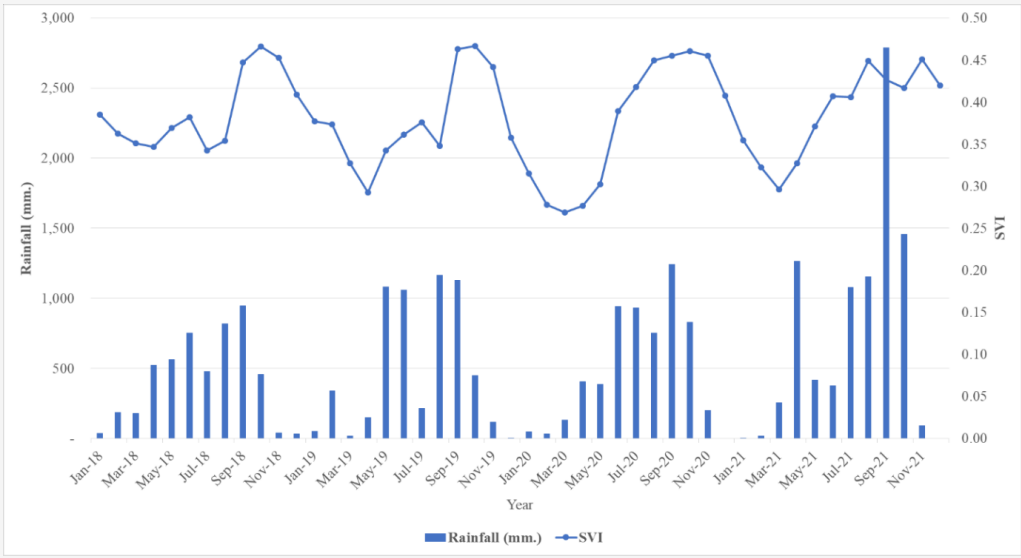

Figure 3: Multi-temporal SVI analysis

Table 4: Statistical correlation analysis from 2018 – 2021

Year	Correlation equation	R^2	Average yearly SVI
2018	y = 4174.9x – 1290.7	0.520	0.389
2019	y = 3686.7x – 1008.4	0.538	0.377
2020	y = 4486x – 1170.0	0.784	0.373
2021	y = 7890.5x – 2302.4	0.606	0.387

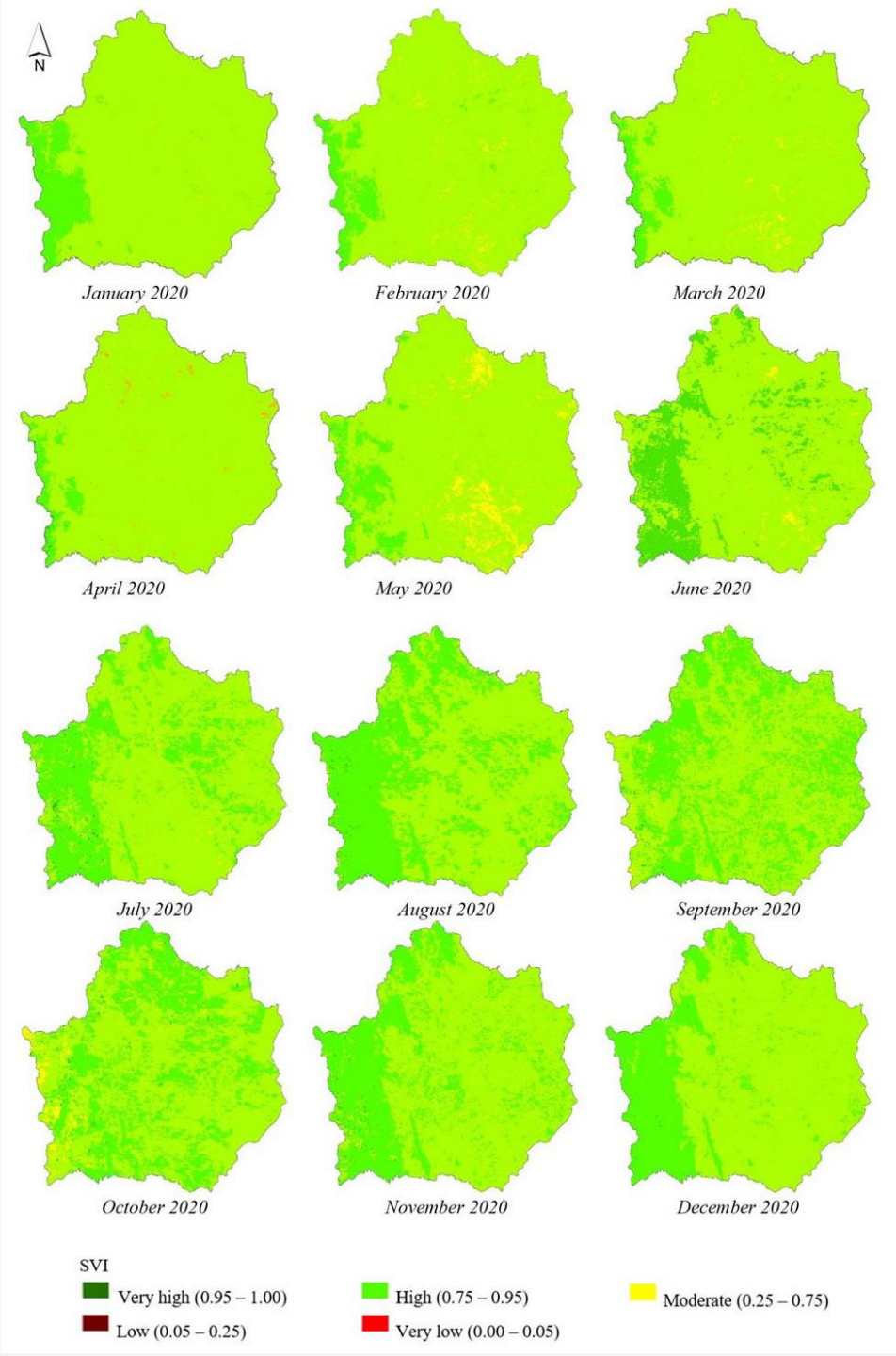

Figure 4: The spatial SVI reflected in 2020

Statistical correlation analysis results between SVI and rainfall in 2018 provided a correlation equation y = 4174.9x – 1290.7 and a coefficient of determination R^2 = 0.520. The statistical correlation analysis result between SVI and rainfall in 2019 provided a correlation equation y = 3686.7x – 1008.4 and a coefficient of determination R^2 = 0.538. The statistical correlation analysis result between SVI and rainfall in 2020 provided a correlation equation y = 4486x – 1170.0 and a coefficient of determination R^2 = 0.784. The statistical correlation analysis result between SVI and rainfall in 2021 provided a correlation equation y = 7890.5x – 2302.4 and a coefficient of determination R^2 = 0.606. The coefficient of determination (R^2) in Table 4 is 0.784, 0.606, 0.538, and 0.520 in 2020, 2021, 2019 and 2018, respectively, based on statistical analysis of the four-year SVI value (independent variable) and monthly rainfall level (dependent variable). Year-over-year positive values for the coefficient of determination (R^2) signify a moderately strong association. Since 2020's annual SVI is lower than previous years', at 0.373, it has a greater statistical value than any other year.

3.5 The Results of Drought Classification from Spatial SVI

Figure 4 shows the correlation equation for this year, which was chosen to explain drought monitoring since it exhibited the highest coefficient of dependence between SVI and average monthly rainfall values found in 2020. Therefore, a 16-day dataset comprising three seasons—summer (February 17 to May 15), rainy (May 17 to October 16), and winter (October 17 to February 16 - was used to analyze the SVI and the average monthly rainfall data. Spatial drought monitoring based SVI was investigated using ArcGIS version 10.8. Monthly SVI fluctuations over time determined by rainfall were found to fall within the low and very low drought classes, with SVI values between 0.00 and 0.25. A moderate drought level was defined as SVI 0.25 to 0.75.

The comparison of SVI at different times of the year revealed variations in the vegetation. The research area's 2020 apparent unique vegetation changes were mirrored in the spatial SVI. Figure 4 shows that early April is when the province of Kamphaeng Phet has the lowest vegetation density. Early in the rainy season, in June, there was a high dispersion of vegetation. May was a month with a high dispersion of vegetation because it was summer.

4. Conclusion

Since NDVI data acquired from MODIS/Terra satellite imagery (MOD13Q1 dataset) was employed simply to analyze and forecast changes of vegetation, SVI approach was further applied to investigate drought based on vegetation probability in varied periods of time. The approach of drought monitoring in provincial scale was developed based on SVI method and monthly rainfall intensity. The lowest average NDVI was found in 2020 in summer period, in accordance with the lowest SVI discovered in the same period of time. The Spatio-temporal analysis between SVI (y) and precipitation data (x) displayed strong correlation of y = 4486x – 1170 equation with R^2 0.739. This could apply to monitor drought in Kamphaeng Phet province. In this paper, the results illustrated that the highest drought incident in 2020 was discovered in Phran Kra Tai district located in the northern and eastern part of province. Inadequate water body together with locating outside the irrigation area could cause the highest drought in this area. The World Meteorology Organization reported that in 2021 it was the hottest year in Thailand. Sixty percent chance of La Nina phenomenon was expected to occur causing more storm during September to November. This could affect “Extreme weather” in 2020. This extreme caused rain to come rapidly and more frequent summer storms can occur in April due to 60 percent precipitation above average. In May, the amount of rainfall began to decrease until June. During July to August, more rain occurred in this period. Noticeably, the beginning of September to October, the amount of rain started to return heavier. 80 mm precipitation was estimated. More than 33 percent of yearly average rainfall resulted in flash flood incidents in the northern region; Mae Hong Son and Chiang Mai province and the upper western region; Tak and Kamphaeng Phet province. To the best of our knowledge, department of disaster prevention and ministry of agriculture and irrigation could deploy this proposed approach for determining and monitoring drought in other parts of Thailand.

Acknowledgements

We would like to express our sincere gratitude to Department of Environmental Science, Faculty of Science, Silpakorn University, Thailand for providing partial financial support. We are also extremely grateful to Kamphaeng Phet Provincial Agriculture and Cooperatives Office, and Thai Meteorological Department (TMD) for contributing data and information.

References

[1] Laosuwan, T., Sangpradid, S., Gomasathit, T. and Rotjanakusol, T., (2016). Application of Remote Sensing Technology for Drought Monitoring in Mahasarakham Province Thailand. *International Journal of Geoinformatics*, Vol. 12(3), 17-25. https://journals.sfu.ca/ijg/index.php/journal/article/view/961.

[2] Zhang, Y., (2015). On the Climate Uncertainty to the Environment Extremes: a Singapore Case and Statistical Approach. *Polish Journal of Environment Studies*, Vol. 24(3), 1413 – 1422. https://doi.org/10.15244/pjoes/31718.

[3] Ghosh, S. K., Garg, P. K. and Prakash, P. S., (2010). *Geospatial Techniques for Drought Assessment and Management*. Proceeding of the 3rd International Conference on Geoinformation Technology for Natural Disaster Management, Chiang Mai, Thailand, Mapping, Managing and Mitigation of Natural Disasters, 19-24.

[4] Ramos Ribeiro, R. R., Sulaiman, S. N., Sieber, S., Angel Trejo-Rangel, M. and Campos, J. F., (2021). Integrated Assessment of Drought Impacts on Rural Areas: The Case of the Chapada Diamantina Region in Brazil. *GeoHazards*, Vol. 2, 442–453. https://doi.org/10.3390/geohazards2040025.

[5] Nightingale, J. M. and Phinn, S. R., (2003). Assessment of Relationships between Precipitation and Satellite Derived Vegetation Condition within South Australia. *Australian Geographical Studies*, Vol. 41, 180. https://doi.org/10.1109/igarss.2001.976835.

[6] Gessner, U., Naeimi, V., Klein, I., Kuenzer, C., Klein, D. and Dech, S., (2013). The Relationship between Precipitation Anomalies and Satellite-Derived Vegetation Activity in Central Asia. *Global and Planetary Change*, Vol. 110, 74-87. https://doi.org/10.1016/j.gloplacha.2012.09.007.

[7] Gomasathit, T., Laosuwan, T., Sangpradid, S. and Rotjanakusol, T., (2015). Assessment of Drought Risk Area in Thung Kula Rong Hai using Geographic Information System and Analytical Hierarchy Process. *International Journal of Geoinformatics*, Vol. 11(2), 21-27. https://journals.sfu.ca/ijg/index.php/journal/article/view/615/406.

[8] Sruthi, S. and Mohammed Aslam, M. A., (2015). Agriculture Drought Analysis Using the NDVI and Land Surface Temperature Data: A Case Study of Raichur District. *Aquatic Procedia*, Vol. 4, 1258-1264. https://doi.org/10.1016/j.aqpro.2015.02.164

[9] Robert, O., Phonekeo, V. and Vaseashta, A., (2008). Semiconducting Gas Sensors, Remote Sensing Technique and Internet GIS for Air Pollution Monitoring in Residential and Industrial Areas. *Functionalized Nanoscale Materials, Devices and Systems*, Chapter 28. Publisher: Springer, 2008, 339-345. https://doi.org/10.1007/978-1-4020-8903-9_28.

[10] Zheentaev, E., (2016). Application of Remote Sensing Technologies for the Environmental Impact Analysis in Kumtor Gold Mining Company. *International Journal of Geoinformatics*, Vol. 12(4), 31-39. https://journals.sfu.ca/ijg/index.php/journal/article/view/989.

[11] Jeefoo, P., (2020). Wildfire Visualization Time Series from 2014-2019 in Phayao Province, Thailand. *International Journal of Geoinformatics*, Vol. 16(4), 29-38. https://journals.sfu.ca/ijg/index.php/journal/article/view/1793.

[12] Buckeridge, D. L., (2002). Making Health Data Maps: A Case Study of a Community/ University Research Collaboration. *Social Science & Medicine,* Vol. 55(7), 1189-206. https://doi.org/10.1016/S0277-9536(01)00246-5.

[13] Maged, N. and Kamel, B., (2004). Towards Evidence-Based, GIS-driven National Spatial Health Information Infrastructure and Surveillance Services in the United Kingdom. *International Journal of Health Geographics*, Vol. 3(1), 1-50. https://doi.org/10.1186%2F1476-072X-3-1.

[14] Vicente-Serrane, S. M., Cabello, D., Tomas-Burguera, M., Martin-Hernandez, N., Beegueria, S., Azorin-Molina, C. and Kenawy, A. E., (2015). Drought Variability and Land Degradation in Semiarid Regions: Assessment Using Remote Sensing Data and Drought Indices (1982-2011). *Remote Sensing*. Vol. 7, 4391-4423. https://doi.org/10.3390/rs70404391

[15] National Disaster Risk Management Plan, 2015. *Department of Disaster Prevention and Mitigation, Ministry of Interior, Thailand.* Available: https://www.disaster.go.th/upload/download/file_attach/584115d64fcee.pdf. [Accessed Dec. 20, 2022].

[16] Kamphaeng Phet database. *Kamphaeng Phet Provincial Office*. Available: https://www.kamphaengphet.go.th/kp/index.php. [Accessed July 31, 2023].

[17] Pachanaparn, C., Jeefoo, P. and Rojanavasu, P., (2022). *Application of Remote Sensing for Drought Monitoring with NDVI-based Standardized Vegetation Index in Nan Province, Thailand*. IEEE – Scopus Indexed Publications the 7th International Conference on Digital Arts, Media and Technology (DAMT) and 5th ECTI Northern Section Conference on Electrical, Electronics, Computer and Telecommunications Engineering (NCON), School of Computer and Information Technology Chiang Rai Rajabhat University, Thailand, 330-335.

[18] Jeefoo, P., (2023). Thai Eastern Economic Corridor Drought Monitoring Using TERRA/MODIS Satellite-based Data. *Geographia Technica*, Vol. 18(2), 123-131. https://doi.org/10.15244/pjoes/94998.

[19] Kriegler, F. J., Malila, W. A., Nalepka, R. F. and Richardson, W., (1969). *Preprocessing Transformations and their Effects on Multispectral Recognition.* Proceeding of the sixth International Symposium on Remote Sensing of Environment, 97-131.

[20] Peters, A. J., Walter-Shea, E. A., Ji, L., Vina, A., Hayes, M. and Svoboda, M. D., (2002). Drought Monitoring with NDVI-Based Standardized Vegetation Index. *Photogram-metric Engineering and Remote Sensing*, Vol. 68(1) 71-75. https://www.asprs .org/wp-content/uploads/pers/2002journal/january/2002_jan_71-75.pdf.

[21] Uttaruk, Y. and Laosuwan, T., (2017). Drought Detection by Application of Remote Sensing Technology and Vegetation Phenology. *Journal Ecological Engineering*, Vol. 18(6), 115-121. https://doi.org/10.12911/22998993/76326.

[22] Jiang, Z., Huete, A., Chen, J., Chen, Y., Li, J., Yan, G. and Zou, Y., (2006). Analysis of NDVI and Scaled Difference Vegetation Index Retrievals of Vegetation Fraction. *Remote Sensing of Environment*, Vol. 101(3), 366-378. https://doi.org/10.1016/j.rse.2006.01.003.

[23] Singh, R. P., Roy, S. and Kogan, F., (2003). Vegetation and Temperature Condition Indices from NOAA AVHRR Data for Drought Monitoring Over India. *Int. J. Remote Sens*., Vol. 24(2), 4393-4402. https://doi.org/10.1080/0143116031000084323.

[24] Wang, J., Rich, P. M. and Price, K. P., 2003. Temporal Responses of NDVI to Precipitation and Temperature in the Central Grate Plains, USA. *Int. J. Remote Sens.*, Vol. 24(11), 2345-2364. https://doi.org/10.1080/01431160210154812.

[25] Thavorntam, W., & Shahnawaz. (2022). Evaluation of Drought in the North of Thailand using Meteorological and Satellite-Based Drought Indices. International Journal of Geoinformatics, 18(5), 13–26. https://doi.org/10.52939/ijg.v18i5.2367

[26] Fensholt R. and Proud, S. R., (2012). Evaluation of Earth Observation Based Global Long-Term Vegetation Trends – Comparing GIMMS and MODIS Global NDVI Time Series. *Remote Sens. Environ*., Vol. 119, 131-147. https://doi.org/10.1016/j.rse.2011.12.015.

[27] Uttaruk, Y. and Laosuwan, T., (2019). Drought Analysis using Satellite-Based Data and Spectral Index in Upper Northeastern Thailand. *Polish Journal of Environment Studies*, Vol. 28(6), 4447-4454. https://doi.org/10.15244/pjoes/94998

[28] Liu, X. and Zhou, J., (2022). Assessment of the Continuous Extreme Drought Events in Namibia during the Last Decade. *Water*, Vol. 13, 2942. https://doi.org/10.3390/w13202942.